Department of Pharmaceutics[1], University of Florida, Gainesville, Florida, Structure Elucidation Group[2], IVAX Drug Research Institute, Budapest, Hungary

Characterization of degradation products of mometasone furoate

S. Sahasranaman[1], M. Issar[1], G. Tóth[2], Gy. Horváth[2], G. Hochhaus[1]

Received October 29, 2003, accepted November 12, 2003

Guenther Hochhaus, Ph.D., Department of Pharmaceutics, College of Pharmacy, Gainesville, FL., 32610 USA
Hochhaus@ufl.edu

Pharmazie 59: 367–373 (2004)

Mometasone furoate (MF) is a synthetic glucocorticoid with anti-inflammatory activity, which is used for the treatment of topical skin disorders, allergic rhinitis and treatment of mild to moderate persistent asthma. The focus of this study is to examine the stability of MF in simulated lung fluid (SLF) and to clearly identify the structure of the degradation products of MF by MS and NMR analysis. Mometasone furoate degradation leads to the formation of two products, D1 and D2 with significant pH dependence. The half-lives for the conversion of MF to D1 and subsequent conversion of D1 to D2 at 37 °C in SLF were 1.3 and 4.8 h respectively. LC-MS and NMR analysis confirmed that D1 is 9,11-epoxide mometasone furoate while D2 represents a new chemical structure that shows cyclization within the C17–C21 region. The biological activity of these degradation products was assessed in rat lung glucocorticoid receptor binding studies. D1 showed 4 fold greater receptor affinity to glucocorticoid receptors compared to dexamethasone. However, the receptor affinity for D2 was a log order lower than that for dexamethasone. The instability of MF in SLF resulted in two degradation products, one of the degradation products showing glucocorticoid receptor activity, the other representing a new cyclized structure whose pharmacological properties have not been described. The biological significance of these degradation products is unknown.

1. Introduction

Mometasone furoate (MF, $C_{27}H_{30}Cl_2O_6$, 9α,21-dichloro-11β,17α-dihydroxy-16α-methylpregna-1,4-diene-3,20-dione 17-(2-furoate), Scheme) is a synthetic glucocorticoid with anti-inflammatory activity. MF has been used in the treatment of topical dermatological disorders (Prakash 1998). As an aqueous nasal spray, MF has been approved

Scheme A schematic degradation pathway for conversion of MF into its degradation products D1 and D2 on incubation of MF ($C_0 = 2.5\ \mu g \cdot mL^{-1}$) in SLF at 37 °C for 72 h. Broken arrows indicate the possible formation of structure E (D3), which was not observed in this study. Structures A, B, D and E represent MF, D1, D2 and D3 respectively. Structure C shows only D-ring of the steroid for presenting the proposed reaction mechanism for the conversion of B to D. A similar reaction mechanism would be possible for formation of structure E from A

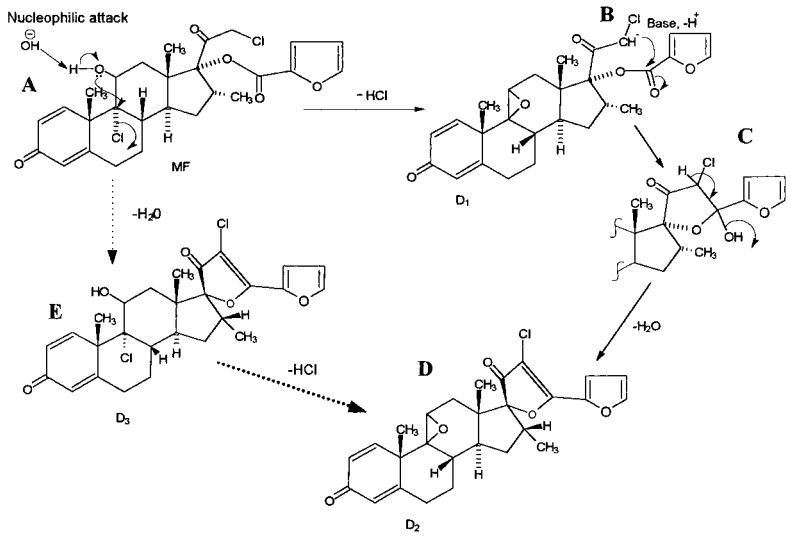

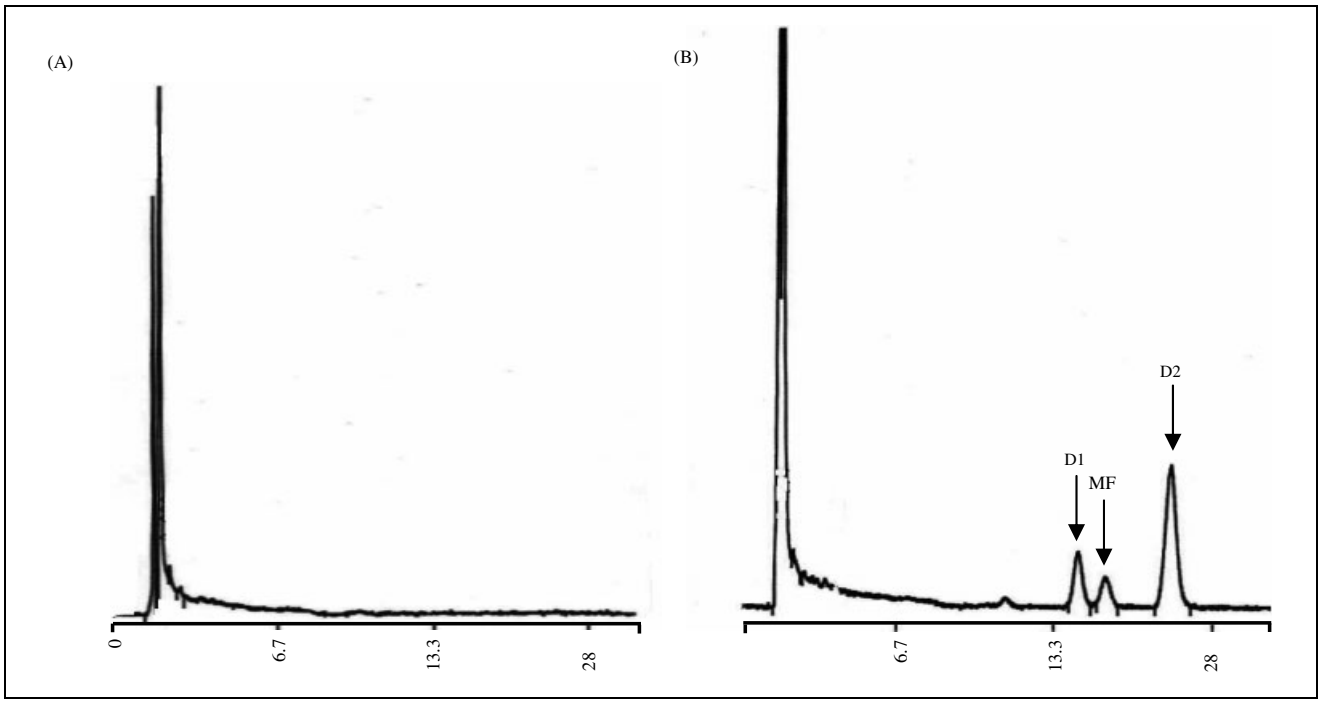

Fig. 1: Representative chromatograms of (a) drug free SLF at 10 h and (b) SLF incubated with MF ($C_0 = 2.5\ \mu g \cdot mL^{-1}$) for 10 h at 37 °C

for the treatment of allergic rhinitis (Onrust 1998). In addition, MF is currently available in the European Union and is being evaluated in the United States as an oral inhalation powder in the treatment of patients with mild-to-moderate persistent asthma (Bernstein et al. 1999; Affrime et al. 2000; Nayak et al. 2000; Sharpe 2001). The above-mentioned studies have shown that MF exhibits a strong anti-inflammatory activity, rapid onset of action, low systemic bioavailability and a favorable ratio between local and systemic side effects**.**

Even though MF has been used extensively, there is very limited information available on the stability of MF in biological tissues/fluids and aqueous systems. Teng and coworkers (Teng et al. 2001) have characterized the degradation of MF in simulated lung fluid (SLF) and have shown that MF is unstable in SLF resulting in three degradation products. They (Teng et al. 2003) have also recently reported the degradation of MF in aqueous systems and have hypothesized the structure of the degradation products based on previous studies conducted with other corticosteroids. The present study aimed to clearly identify the structures of these degradation products by LC-MS and NMR analysis. It was of further interest to assess their potential biological activity, by performing rat lung glucocorticoid receptor binding studies, because of the possibility of these degradation products being formed *in vivo*.

2. Investigations, results and discussion

2.1. Stability of MF in SLF

In agreement with findings of Teng and coworkers (Teng et al. 2001), incubation of MF ($C_0 = 2.5\ \mu g \cdot mL^{-1}$) in SLF at 37 °C and subsequent HPLC analysis of the incubation mixture suggests the formation of two major degradation products, named D1 and D2 (Fig. 1). The concentration-time profiles of MF, D1 and D2 (Fig. 2) indicate that more than 90% of MF undergoes conversion to either D1 and or D2 at the end of 4 h of incubation with D1 being formed faster than D2. After 12 h, the majority of the starting material entered the D2 pool with MF being undetectable; therefore one can conclude that D1 seems to be converted into D2. Consequently, it appears that MF is first converted into D1, which is subsequently converted into D2 (see Fig. 2). Indeed fitting of the data to this model resulted in satisfying fits; small under or overestimations might be related to the changes of the pH during incubation, which affected the degradation rate constants (see below). The apparent degradation rate constant ($k_1 = 0.52\ h^{-1}$) for the conversion of MF to D1 was found to be nearly 4 times higher than the degradation rate constant ($k_2 = 0.143\ h^{-1}$) for the conversion of D1 to D2. The degradation half-life for MF was found to be 1.3 h and the half-life of D1 was 4.8 h. Thus, degradation profile shown in the upper part of the Scheme (denoted by solid lines) is supported by the data. This suggests that there are qualitative and quantitative differences between this study and that conducted by Teng et al. (2001) who reported the formation of another minor degradation product, D3. However, D3 is not seen in this study even

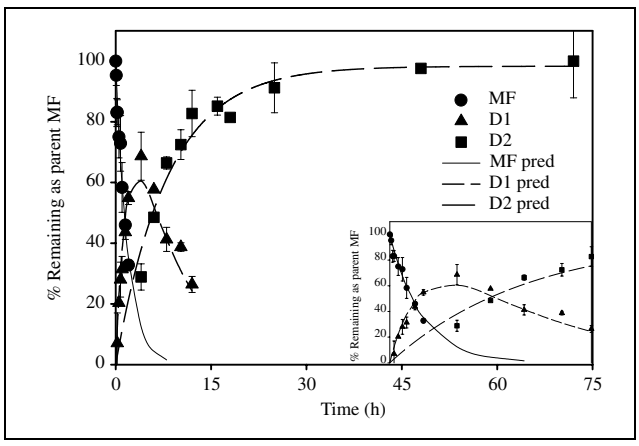

Fig. 2: Graphical representation showing nonlinear curve fitting of the concentration-time data of MF and its degradation products D1 and D2 generated after incubation of MF in SLF at 37 °C for 72 h (N = 2). The inset graph shows the expanded time scale upto 12 h

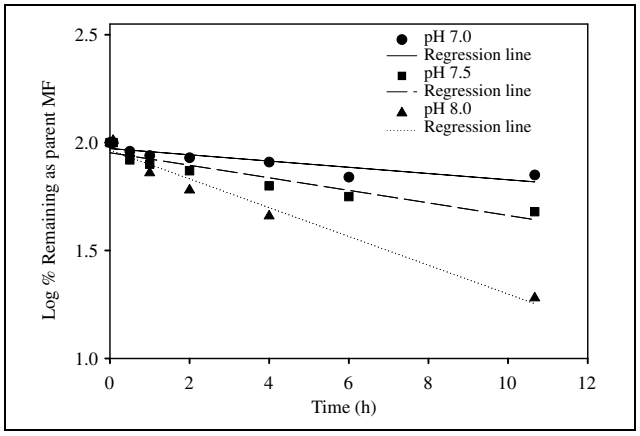

Fig. 3: The degradation profiles for MF ($C_0 = 2.5$ μg mL^{-1}) in phosphate buffer at pH 7.0, 7.5 and 8.0 at 37 °C

though a more sensitive assay was used. The half-life of MF in SLF in this study was found to be 3.5 times shorter compared to the half-life reported by Teng et al. The concentration of D2 after 72 h in this study was approximately 80% as that of parent MF compared to 30% by Teng et al. (2001). It might be speculated that differences in the buffer composition, ionic strength or other factors might be the reason for the somewhat different degradation pathways.

The rate of degradation of MF was found to vary as a function of pH of the buffer solution. During incubation at 37 °C, the starting pH of the SLF buffer solution was 7.4 that gradually became alkaline (pH 8.9) at the end of 72 h. The pH shift of the SLF buffer solution was also monitored at ambient temperature (25 °C) and it was observed that the pH gradually changed from 7.4 to 7.9 in 4 h and was distinctly alkaline (pH 9.1) at the end of 72 h. It is proposed that the buffer system gradually turns alkaline due to the loss of acid (loss of CO_2 from the buffer system). This could be due to the presence of sodium bicarbonate in the buffer (~30 m*M*) and a low buffering capacity of phosphate buffer (~1 m*M*) present in the SLF. However, the cause of the pH raise during incubation is uncertain.

In order to assess the pH dependence, degradation process experiments were conducted in 50 mM K_2HPO_4 buffer at three different pH values (pH 7.0, 7.5 and 8.0, Fig. 3). The degradation rate of MF increased with increased pH. The degradation rate constants were 0.03, 0.06, and 0.15 h^{-1} for pH 7.0, 7.5 and 8.0 respectively. The results in this study are in agreement with the report by Teng et al. (2003) that was recently published while this manuscript was in preparation. It may be noted that the degradation rate constant of MF (0.52 h^{-1}) in SLF was higher than the degradation rate constant observed in 50 mM K_2HPO_4 buffer at pH 8.0. This suggests that ionic effects, because of the presence of salts in the composition of SLF, play a significant role in the degradation of MF.

2.2. MS analysis of the MF and its degradation products

Based on the ESI+ mass spectra (Table 1), the molecular formulae of D1 and D2 agree with the general structures $C_{27}H_{29}ClO_6$ and $C_{27}H_{27}ClO_5$ respectively. The molecular masses of D1 and D2 are in agreement with those reported by Teng et al. (2003). The mass spectra data indicated a loss of HCl for D1 when compared with MF.

Table 1: Electrospray ionization mass spectral data* of MF and its degradation products

Compound	MF	D1	D2
Molecular formula	$C_{27}H_{30}Cl_2O_6$	$C_{27}H_{29}ClO_6$	$C_{27}H_{27}ClO_5$
$[MH]^+$	521 (100)***	485 (15)***	467 (60)***
$[MH]^+$ (^{37}Cl isotope)	523 (70)	487 (5)	469 (20)
$[MH + Na + CH_3OH]$	555 (10)**	539 (10)**	521 (100)**
$[M + Na]^+$	543 (30)**	507 (100)**	489 (35)**
$[MH-H_2O]^+$	503 (10)**	–	–
$[MH-HCl]^+$	485 (15)**	–	–
Others	441 (5) 413 (15)	413 (5)	413 (10)

* Listed are m/z. % relative abundance to nearest 5% is given in parenthesis
** Corresponding ^{37}Cl isotope ion was also observed
*** This was determined to be the parent compound based on independent chemical ionization mass spectrometry analysis (data not shown)

Similarly, D2 differed from D1 by a loss of H_2O. The presence of only one chlorine atom in D1 and D2 was confirmed by the relative abundance of ^{37}Cl isotope in D1 and D2 (35%) compared to the relative abundance in MF (70%) that has two chlorine atoms.

2.3. NMR analysis of the degradation products

The structure determination of MF was based on the NMR spectral assignments, confirmed by DEPT, two-dimensional ^{1}H,^{1}H-COSY, ^{1}H,^{13}C-HSQC, ^{1}H,^{13}C-HMBC and one-dimensional selective NOESY experiments. The ^{1}H and ^{13}C chemical shifts, characteristic proton-proton couplings (Hz), ^{13}C,^{1}H long-range correlations (HMBC) and ^{1}H,^{1}H steric proximities (NOE) are summarized in Table 2.

The ^{1}H,^{1}H-COSY spectrum gave the geminal and vicinal proton-proton connectivities and the ^{1}H,^{13}C-HSQC provided the chemical shifts of the one-bonded coupled ^{13}C-^{1}H nuclei. The ^{1}H,^{13}C-HMBC experiment was used for the assignment of the quaternary carbons since the cross peaks revealed the two- and three-bond correlations between protons and carbons. The stereochemistry of the steroid skeleton and the substituents, the determination of the α- and β-positions of the protons were achieved on the basis of the one-dimensional NOESY experiments irradiating the Me-16, Me-18 and Me-19 protons. These experiments marked out the protons that are located in a distance less than 5 Å from the irradiated protons.

NMR analysis on D1 could not be performed satisfactorily since the quantity of D1 generated was insufficient because of its inherent instability. Structural determination of D2 was based on NMR spectral assignments which were confirmed by two-dimensional ^{1}H,^{13}C-HSQC, ^{1}H,^{13}C-HMBC and one-dimensional selective NOSEY experiments. The ^{1}H and ^{13}C chemical shifts, characteristic proton-proton couplings (Hz), ^{13}C,^{1}H long-range correlations (HMBC) and ^{1}H,^{1}H steric proximities (NOE) are summarized in Table 3.

The ^{1}H,^{13}C-HSQC provided the chemical shifts of the one-bonded ^{13}C-^{1}H nuclei. The ^{1}H,^{13}C-HMBC experiment was used for the assignment of the quaternary carbons since the cross peaks revealed the two- and three-bond correlations between protons and carbons. The stereochemistry of the steroid skeleton and the substituents, the determination of the α- and β-positions of the protons were achieved on the basis of their coupling pattern and utilizing the results of the one-dimensional NOSEY experiment irradiating the Me-18 protons. This measurement

Table 2: ^{1}H and 13C chemical shifts, characteristic couplings (Hz), ^{13}C, ^{1}H long-range correlations (HMBC) and 1H,1H steric proximities NOE of compound MF

		$\delta^{1}H$	$\delta^{13}C$	HMBC (^{13}C partner)	NOE
1		7.18 d (10.0)	151.5	3, 5	
2		6.37 dd (10.0)	129.8	10	
3		–	186.3		
4		6.l3 dd (2.0, 1.5)	125.3	1, 6, 10	
5		–	165.2		
6	β	2.66 m	30.6	4, 5	
	α	2.43 ddd (14.3, 4.3, ∼1)		4, 5, 8, 10	
7	β/α	1.81 m	27.2		
8		2.64 m	34.5		
9		–	82.8		
10		–	49.8		
11	α	4.64 dd (3.6, 2.8)	75.2		
HO-11	β	1.76 d (2.8)	–		
12	β	1.72 dd (14.2, 2.5)	36.7	9, 13, 14, 17	
	α	2.94 dd (14.2, 3.6)			
13		–	48.9		
14	α	2.66 m	43.8		
15	β	1.92 m	32.9		
	α	1.33 ddd (11.3, 7.6, 3.5)			
16	β	3.47 m	35.8		
Me-16	α	0.99 (7.1)	16.7	15, 16, 17	15α, 16
17		–	97.4		
18	α	1.15 s	17.7	12, 13, 14, 17	8, HO-11, 120, 15β, 16, 21
19	α	1.68s	24.5	1, 5, 9, 10	1, 6β, 8
20		–	196.8		
21		4.14s	44.7	20	
OC=O		–	158.1		
f2		–	143.0		
f3		7.25 dd (3.6, 0.7)	119.6		
f4		6.54 dd (3.6, 1.7)	112.3		
F5		7.63 dd (1.7, 0.7)	147.7	f2, f3	

Table 3: ^{1}H and ^{13}C chemical shifts, characteristic couplings (Hz), ^{13}C, ^{1}H and long-range correlations (HMBC) of compound D2

		$\delta^{1}H$	$\delta^{13}C$	HMBC (^{13}C partner)
1		6.57 d (10.4)	151.9	3, 5
2		6.18 dd (10.4, 1.8)–∼	128.1	10
3		–	186.0	
4		6.20 d (1.8)	125.1	1, 6, 10
5		–	164.7	
6	β	2.71 dddd (15.5, 11.3, 5.5, 1.7)	29.3	4, 5
	α	2.53 dt (15.5, 5.3)		4, 5, 8, 10
7	β	2.41 m	30.5	
	α	1.53 m		
8	β	2.36 m	34.2	
9		–	66.1	
10		–	44.1	
11	α	3.13 t (2.3)	62.4	
12	β	1.71 d (2.3)	30.4	9, 13, 14, 17
	α	1.71 d (2.3)		
13			49.7	
14	α	1.89 m	50.0	
15	β		34.2	
16	β	2.87 m	39.5	
Me-16	α	0.88 d (7.1)	13.9	15, 16, 17
17		–	100.1	
18	β	1.27 s	15.8	12, 13, 14, 17
19	β	1.46 s	23.7	1, 5, 9, 10
20		–	194.6	
21		–	106.7	20
OC=O		–	166.8	
f2		–	142.8	
f3		7.50 dd (3.8,0.7)	118.8	
f4		6.68 dd (3.8, 1.8)	112.9	
f5		7.61 dd (1.8, 0.7)	147.0	f2, f3

gave well-defined NOE responses on H_{β}-16, H-8, H_2-12 protons, and a rather small one on H_{β}-15.

The ^{13}C spectrum shows the absence of the C21-H_2 methylene group and the corresponding carbon signal appeared at δ106.7. This clearly indicates that condensation took place between the ester carbonyl and the above-mentioned methylene resulting in a new, five-member spiro-ring at position C17. The very high value of the one-bond coupling ^{1}J(H-11, C-11) = 175 Hz, unambiguously prove the presence of an epoxide group in the "C" ring.

As a result of the MS and NMR analysis, the structure of D2 is shown in the Scheme. This structure of D2 is different from the structure proposed by Teng et al. (2003) who hypothesized a furoate-ester migration between C17 and C21 positions. Even though such ester migrations have been reported for other steroids like betamethasone 17-valerate (Bundgaard 1980), beclomethasone monopropionate (Foe et al. 1998) and hydrocortisone butyrate (Yip et al. 1983), this phenomenon cannot be expected to happen in steroids like MF that have a halogen atom at C21 (Mori et al. 1994; Prakash 1998). Based on these LC-MS and NMR analyses, the authors believe the proposed structure for D2 in this study is accurate and unambiguous.

As mentioned earlier, D2 appears to be formed upon degradation of D1. Based on this hypothesis, the structure of D2 and the MS analysis of D1, D1 is 9, 11-epoxide mometasone furoate (Scheme). The complete degradation pathway of MF in SLF is summarized in the Scheme. The results of this study do not completely preclude the formation of compound D3 (pathway shown by dashed lines in the Scheme) under somewhat different experimental conditions even though the formation of this compound is not seen in this study.

2.4. Glucocorticoid receptor binding of MF and its degradation products

The relative binding affinities of MF and the isolated degradation products D1 and D2 were determined in a competition binding experiment in rat lung cytosol. Table 4 compares the average IC_{50} values and relative binding affinity (RBA) values for dexamethasone, MF, D1 and D2. The data shows that MF is 29 times more potent than dexamethasone. The binding affinity of D1 to the rat glucocorticoid receptor was 4 times higher than dexamethasone. The IC_{50} value of the degradation product D2 could not be determined precisely as D2 did not show binding to the glucocorticoid receptors in the concentration range studied.

Bledsoe et al. (2002) recently determined the crystal structure of the glucocorticoid receptor ligand-binding domain in a ternary complex with dexamethasone. The glucocorticoid receptor ligand binding domain has a unique side pocket that may account for the selectivity of glucocorticoids with substituents at the C-17α position (Bledsoe et al. 2002; Necela 2003). This may explain the strong binding of MF and D1, which have a furoate moiety at the C17α position, to the glucocorticoid receptor. However, the structural changes in D2, with its condensation between the furoate ester carbonyl and the methylene group at C21 leading to the formation of the five-member ring, seems to interfere with the interaction of the steroid with the receptor in this region of the receptor pocket resulting in a significantly reduced binding affinity of D2.

The competition curves for dexamethasone, MF, D1 and D2 are shown in Fig. 4. In all binding experiments, nonlinear curve fitting revealed slope factors (Hill coefficient) for dexamethasone, MF and D1 were close to 1. The RBA value for MF in this study is slightly higher but in agreement with earlier reported values (Dahlberg et al. 1984). 9,11-Epoxide-mometasone furoate (D1) has a reduced binding affinity of 433, but this RBA value is comparable to and even greater than many of the currently used inhaled corticosteroids like flunisolide (RBA 180), triamcinolone acetonide (RBA 233) and budesonide (RBA 935) (Würthwein et al. 1992). These results also indicate that the presence of an 11β-OH-group is favorable but not absolutely necessary for receptor binding. The binding affinity of 9,11-epoxide-MF compared to MF in this study to the receptor in rat lung is in agreement with the values reported by Isogai et al. (1993) for the glucocorticoid receptor of rat skin.

In summary, MF is unstable in aqueous systems resulting in two epoxidated degradation products. One of the degradation products showing glucocorticoid receptor activity, the other representing a new cyclized structure whose pharmacological and toxicological properties have not been described. These instabilities are not typically seen for glucocorticoids that do not have the specific features of MF (furoate group in C17, Cl group at C21 and C9).

Table 4: Relative binding affinities (RBA) to the glucocorticoid receptor of rat lung tissue

Compound	Hill coefficent (N)	IC_{50} (μM)	RBA
Dexamethasone	1	0.046 ± 0.01	100
Mometasone furoate	1	0.0016 ± 0.0001	2938
Metabolite D1	1	0.011 ± 0.0002	433
Metabolite D2*	1	∼0.290 ± 0.034	∼15.8

* Indicates rough estimates of IC_{50} obtained by fixing the hill coefficient to 1

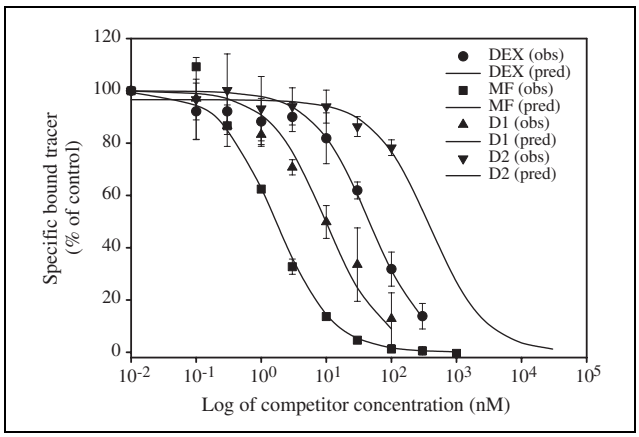

Fig. 4: Competitive binding experiments to the glucocorticoid receptors in rat lung cytosol. Nonlinear regression of non-transformed data was used for the determination of IC_{50} values of dexamethasone, MF, degradation products D1 and D2. An approximate IC_{50} value for D2 was determined to be 0.29 ± 0.034 μM (n = 2). The estimated parameters for D2 were then used to predict bound tracer at competitor concentrations higher than 0.3 μM. The hill coefficient was fixed to 1

Further studies need to investigate whether these degradation products also occur *in vivo* or in aqueous based MF formulations.

3. Experimental

3.1. Chemicals

Mometasone furoate (MF) was purchased from USP (Rockville, MD). Dexamethasone was purchased from Sigma Chemicals Co (St Louis, MO). ^{3}H-Triamcinolone acetonide (specific activity 38 Ci · mmol^{-1}) was purchased from Perkin Elmer Life Sciences (Boston, MA). The degradation products of MF: D1 and D2 were isolated and purified using HPLC and solid phase extraction in our laboratory. All other chemicals and solvents were obtained from Sigma Chemicals Co. (St Louis, MO) and Fisher Scientific Co. (Cincinnati, OH).

3.2. Stability of MF in simulated lung fluid (SLF)

Composition of the simulated lung fluid buffer was adopted from the report of Kalkwarf (1983). In brief, SLF comprised of 0.2033 g $MgCl_2 \cdot 6\,H_2O$ (1 *m*M), 6.019 g NaCl (103 *m*M), 0.2982 g KCl (4 *m*M), 0.2680 g $Na_2HPO_4 \cdot 7$ H2O (1 *m*M), 0.0710 g Na_2SO_4 (0.5 *m*M), 0.3676 g $CaCl_2 \cdot 2\,H_2O$ (2.5 *m*M), 0.9526 g $NaH_3C_2O_2 \cdot 3\,H_2O$ (7 *m*M), 2.6043 g $NaHCO_3$, (31 *m*M) and 0.0970 g $Na_3H_3C_6O_7 \cdot 2\,H_2O$ (0.33 *m*M) dissolved in one liter of distilled water. The pH of the SLF buffer solution was adjusted to 7.4 using dilute HCl (20% v/v). 10 ml of the SLF was pre-incubated at 37 °C for 10 min, and spiked with MF (1 mg · mL^{-1} stock solution) to achieve a concentration of 2.5 g · mL^{-1}. Blank buffer was used in a control experiment. 500 μL aliquot samples were withdrawn at 0, 5, 10, 15, 30, 45 min and then at 1, 1.5, 2, 4, 6, 7, 24, 48 and 72 h into pre-chilled tubes and the samples were diluted with 500 μL of mobile phase (63 : 37% v/v MeOH−H_2O). The samples were analyzed by HPLC-UV.

A LDC/Milton Roy CM4000 multiple solvent delivery system using a Milton Roy SM 4000 programmable wavelength detector set at λ_{max} 254 nm, a CR-3A Chromatopac integrator (Shimadzu Corporation, Japan) and an automatic injector (Perkin Elmer, Boston, MA) was used as HPLC system. Chromatographic separation of the analytes was achieved on Waters 5-m symmetry RP-18 (150 × 4.6 mm i.d) column (Milford, MA) preceded with a guard column (10 × 4.6 mm i.d, filled with reverse phase pre-column material) using a mobile phase of 63 : 37% v/v methanol-water at a flow rate of 1 ml.

Calibration curves based on MF peak areas over the concentration range of 0.125 to 5.0 g · mL^{-1} using unweighted least squares linear regression analysis resulted in r^2 values of at least 0.999. The limit of quantification of the assay was 0.125 g · mL^{-1}. The good reproducibility of the system allowed quantification without an internal standard as potential internal standards either cross-eluted with degradation products or were unstable in the buffer systems used.

Because of the lack suitable standards of D1 and D2, quantification of the degradation products was based on the assumption that the molar absorptivities were similar to that of MF. Results for MF and degradation products are presented in M and expressed in % of MF starting concentrations in graphical representations.

The concentration-time data obtained for MF and its degradation products were fitted using SCIENTIST™ software (version 2.0, Micromath®, Salt Lake City, UT) using the model shown in the Scheme. Alternative degradation pathways (Scheme) allowing first for the cyclization of MF followed by epoxide formation was not indicated by the number of degradation products identified. The half-lives for the different compounds were calculated using the equation (1):

$$T_{1/2} = \frac{0.693}{k_{app}} \quad (1)$$

where k_{app} is the apparent degradation constant for that compound.

3.3. Effect of pH on stability of MF in SLF

To assess the pH dependence, degradation process experiments were conducted in 50 mM K_2HPO_4 buffer at three different pH values (pH 7.0, 7.5 and 8.0). A fifty times higher buffer strength (compared to SLF) of K_2HPO_4 was selected to improve the buffering capacity. The pH of the buffer at the higher buffer strength did not change over an incubation period of 24 h at 37 °C. MF at a concentration of 2.5 $\mu g \cdot mL^{-1}$ (4.8 M) was incubated at 37 °C in a shaker bath. 200 µL aliquot samples were withdrawn at 0, 5, 30, min and then at 1, 2, 4, 6, 8, and 10.6 h into pre-chilled tubes and the samples were diluted with 200 µL of mobile phase (63 : 37 MeOH−H_2O). The samples were analyzed using HPLC-UV as described above.

3.4. Isolation of the degradation products formed during incubation of MF in SLF

For the purpose of isolation of degradation products, 4 vials containing 10 mL of SLF buffer were spiked with MF (1 $mg \cdot mL^{-1}$ stock solution) to give a concentration of 10 $g \cdot mL^{-1}$. After incubation, the contents of the vials were pooled and 1 mL aliquots of the spiked SLF were transferred to individual solid-phase extraction (SPE) cartridges and extracted as reported previously (Krishnaswami et al. 2000). The extracted and reconstituted samples were injected onto the HPLC and the peaks corresponding to the various degradation products were collected using a fraction collector (Gilson Model 203, Middleton, WI). Several HPLC runs had to be performed to purify sufficient amount of material. The fractions corresponding to each degradation product were pooled and extracted using the SPE procedure described above. Purity (greater than 95%) and content of the isolated degradation products were determined by HPLC. The isolated fractions were analyzed by MS and NMR for structure determinations (see below). In addition, the activity of these isolated degradation products was assessed in glucocorticoid receptor binding experiments (see below).

3.5. Mass spectrometry of MF and its degradation products

LC-MS analysis was used to identify the molecular mass of the degradation products of MF. The chromatographic separation of the analytes was achieved on a Waters 5-µm symmetry RP-18 (50 × 4.6 mm i.d) column (Milford, MA) with an aqueous mobile phase containing 70 : 30% v/v MeOH−H_2O and flow rate of 0.3 $ml \cdot min^{-1}$. The LC system was connected to a Micromass Quattro-LC-Z (Beverly, MA) triple quadrupole mass spectrometer equipped with ES+ (electro-spray) ion source. The source temperature was set to 120 °C and the ES probe temperature was 400 °C. Capillary and cone voltages were set to 3kV and 25 V respectively. The samples were detected using a full scan mode. The mass spectrometer was linked to a Perkin Elmer ISS-200 auto sampler via a contact closure and the operation was controlled by computer software MASSLYNX 3.1.

3.6. Structure elucidation of degradation products using NMR

The NMR spectra were recorded in $CDCl_3$ at room temperature using Shigemi sample tubes (180 µl) on Bruker Avance-500 spectrometer at 500.13/125.7 MHz. The pulse programs were taken from Bruker software library.

3.7. Glucocorticoid receptor binding assay experiments in rat lung cytosol

The various dilutions for MF (0.01, 0.03, 0.1, 0.3, 1.0, 3.0, 10.0, 30.0, 100 µM) were prepared in methanol. Dilutions for degradation product D1 and dexamethasone (0.001, 0.003, 0.01, 0.03, 0.1, 0.3, 1.0 µM) and degradation product D2 (0.001, 0.003, 0.01, 0.03, 0.1, 0.3, 1.0, 0.3 µM) were also prepared in methanol.

The animal protocol was approved by the local Institutional Animal Care and Use Committee (IACUC) at the University of Florida, Gainesville, Florida. *Sprague Dawley* rats (250 ± 25 g) were obtained from Harlan (Indianapolis, IN). The rats were anesthetized using a cocktail mixture of ketamine, xylazine and acepromazine (3 : 3 : 1 v/v) and were decapitated. The lungs were removed and homogenized in 8 volumes of ice-cold incubation buffer (10 mM Tris/HCl, 10 mM sodium molybdate, 2 mM 1,4-dithioerythritol). The homogenate was incubated with 5% w/v charcoal suspension (in deionized water) for 10 min. The homogenate was then centrifuged for 20 min at 40,000 × *g* in J2 rotor of Beckman centrifuge to obtain the cytosol. Fresh cytosol was prepared and used for all the individual experiments.

10 nM of ^{3}H-labeled triamcinolone acetonide (TA) solution was used as a tracer, based on previous saturation binding experiments performed in our laboratory (data not shown). 20 µL of the drug solution in methanol was added to pre-chilled tubes. Blank methanol was used for the determination of total binding. Non-specific binding was determined after addition of 20 µL of 100 µM unlabeled triamcinolone acetonide (10 µM in the final incubation mixture). 20 µL of 100 n*M* ^{3}H-triamcinolone acetonide solution (10 nM in final incubation mixture) was then added. 160 µL of the lung cytosol was added and the tubes were vortexed and incubated at 4 °C for 24 h. After the incubation, 200 µL of 5% w/v charcoal suspension (in water) was added to the tubes to remove the excess unbound radioactivity. The tubes were vortexed and 300 µL of the supernatant was transferred to the scintillation vials. 5 mL of the scintillation cocktail was added and the scintillation vials were read in a liquid scintillation counter (Beckman Instruments LS 5000 TD, Palo Alto, CA). The stability of MF and the degradation products under the incubation conditions (4 °C), was demonstrated by HPLC after extraction of the incubation mixture by solid phase extraction.

The data obtained were fitted by SCIENTIST™ (Micromath, Salt Lake City, UT) using the following E_{max} model to obtain the estimates of B_{max} and IC_{50}.

$$DPM = B_{max} - B_{max}\frac{C^N}{IC_{50}^N + C^N} + NS \quad (2)$$

where DPM represents the total tracer binding obtained at any given competitor concentration, NS represents non-specific binding and N the Hill coefficient. B_{max} is the specific binding by the ligand in the absence of competitor.

The IC_{50} obtained for dexamethasone ($IC_{50,dex}$) was used to calculate the relative binding affinity (RBA_{test}) of the test compound form its IC_{50} value ($IC_{50,test}$) as:

$$RBA_{test} = \frac{IC_{50,\,dex}}{IC_{50,\,test}} \times 100\,. \quad (3)$$

The stability of MF and its degradation products in the rat lung cytosol at 4 °C was checked by spiking the compounds separately in cytosol and incubating the samples for 24 h at 4 °C. Blank cytosol was considered as control. One set of spiked cytosol was analyzed at zero time and the other set was analyzed after 24 h (time period of incubation).

Acknowledgement: We would like to thank AstraZeneca for their financial support of this study.

This research paper was presented at the 4th Conference on Retrometabolism Based Drug Design and Targeting, May 11–14, 2003, Palm Coast, Florida, USA.

References

Affrime MB, Cuss F et al. (2000) Bioavailability and metabolism of mometasone furoate following administration by metered-dose and dry-powder inhalers in healthy human volunteers. J Clin Pharmacol 40: 1227–1236.

Bernstein DI, Berkowitz RB et al. (1999) Dose-ranging study of a new steroid for asthma: mometasone furoate dry powder inhaler. Respir Med 93: 603–612.

Bledsoe RK, Montana VG et al. (2002) Crystal structure of the glucocorticoid receptor ligand binding domain reveals a novel mode of receptor dimerization and coactivator recognition. Cell 110: 93–105.

Bundgaard H, Hansen J (1980) Studies on the stability of corticosteroids VI. Kinetics of the rearrangement of betamethasone-17-valerate to the 21-valerate ester in aqueous solution. Int J Pharm 7: 197–203.

Dahlberg E, Thalen A et al. (1984) Correlation between chemical structure, receptor binding, and biological activity of some novel, highly active, 16 alpha, 17 alpha-acetal-substituted glucocorticoids. Mol Pharmacol 25: 70–78.

Foe K, Brown KF et al. (1998) Decomposition of beclomethasone propionate esters in human plasma. Biopharm Drug Dispos 19: 1–8.

Isogai M, Shimizu H et al. (1993) Binding affinities of mometasone furoate and related compounds including its metabolites for the glucocorticoid receptor of rat skin tissue. J Steroid Biochem Mol Biol 44: 141–145.

Kalkwarf DR (1983) Dissolution rates of uranium compounds in simulated lung fluid. Sci Total Environ 28: 405–414.

Krishnaswami S, Mollmann H et al. (2000) A sensitive LC-MS/MS method for the quantification of fluticasone propionate in human plasma. J Pharm Biomed Anal 22: 123–129.

Mori M, Pimpinelli N et al. (1994) Topical corticosteroids and unwanted local effects. Improving the benefit/risk ratio. Drug Safety 10: 406–412.

Nayak AS, Banov C et al. (2000) Once-daily mometasone furoate dry powder inhaler in the treatment of patients with persistent asthma. Ann Allergy Asthma Immunol 84: 417–424.

Necela BM, Cidlowski JA (2003) Crystallization of the human glucocorticoid receptor ligand binding domain: a step towards selective glucocorticoids. Trends Pharmacol Sci 24: 58–61.
Onrust SV, Lamb HM (1998) Mometasone furoate. A review of its intranasal use in allergic rhinitis. Drugs 56: 725–745.
Prakash A, Benfield P (1998) Topical mometasone. A review of its pharmacological properties and therapeutic use in the treatment of dermatological disorders. Drugs 55: 145–163.
Sharpe M, Jarvis B (2001) Inhaled mometasone furoate: a review of its use in adults and adolescents with persistent asthma. Drugs 61: 1325–1350.
Teng XW, Cutler DC et al. (2003) Degradation kinetics of mometasone furoate in aqueous systems. Int J Pharm 259: 129–141.
Teng XW, Foe K et al. (2001) High-performance liquid chromatographic analysis of mometasone furoate and its degradation products: application to in vitro degradation studies. J Pharm Biomed Anal 26: 313–319.
Würthwein G, Rohdewald P (1992) Lipophilicity and receptor affinity of glucocorticoids. Pharm Ztg Wissensch 5/137: 161–167.
Yip YW, Li Wan Po A Rodewald P (1983) Kinetics of decomposition and formulation of hydrocortisone butyrate in semiaqueous and gel systems. J Pharm Sci 72: 776–781.